Project 1:

Wing design and modelling

UPC ESEIAAT - MUEA

Subject: 220351 - ADVANCED AEROELASTICITY

Author:

Cornudella Quer, Pau

Data:

November 24, 2025

1 Introduction and objectives

This project focuses on the structural and aeroelastic design of a glider wing under a series of predefined constraints, specifically;

- The wing must incorporate a NACA0010 airfoil, with a root chord of $c_0 = 0.85$ m.
- The wing must be attached to the fuselage at a distance $r_0 = 0.34$ m from the glider's symmetry plane ($y = 0$).
- The structure must be entirely made of aluminium, with a density $\rho = 2300$ kg/m^3, elastic modulus $E = 69$ GPa, and Poisson's ratio $\nu = 0.3$.
- The wing's dihedral angle must remain zero, and the shear centre must stay aligned along a straight line perpendicular to the $y = 0$ plane.

Beyond these restrictions, the student is free to select the wing span b, the taper ratio λ, the angle of attack α, the free-stream velocity U_∞, and the internal profile geometry and thickness.

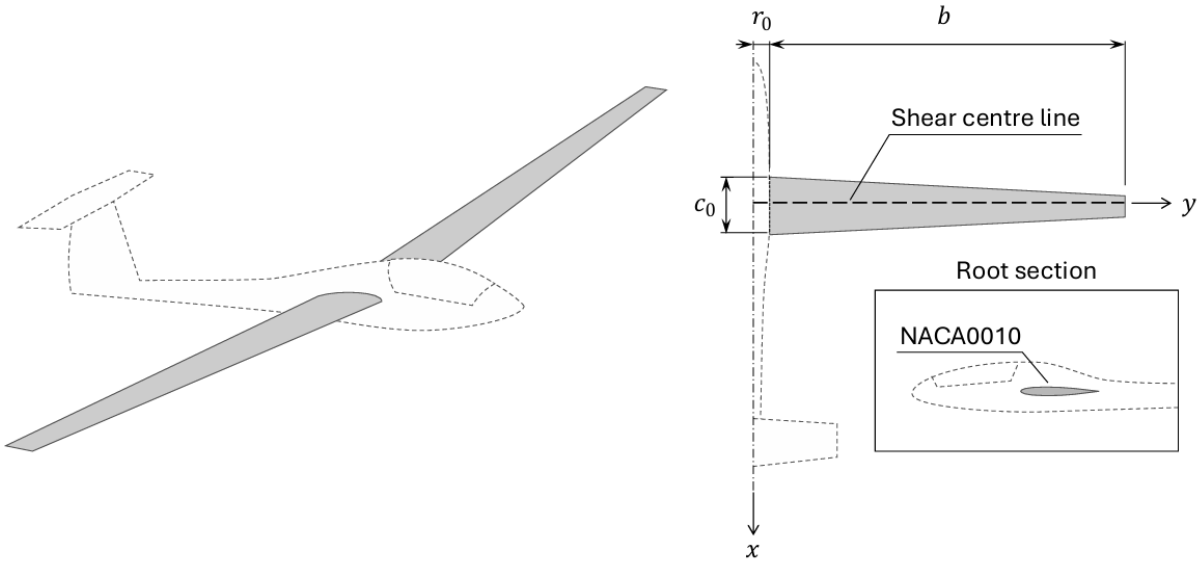

Figure 1: Schematic representation of the glider and the wing design.

The wing is analyzed considering a beam model, in which the cross-sectional properties vary along the span. This includes the bending and torsional stiffnesses, mass per unit length, inertia terms, and the location of the shear centre.

Afterwards, the aerodynamic loads are obtained through the Doublet Lattice Method (DLM), which provides the pressure coefficient C_p distribution along the wing. From this, the global lift distribution L, lift-to-mass ratio C_L/μ, and the stress-to-mass ratio C_σ/μ are extracted.

In summary, the main goals of the project are:

1. To design the wing's geometry and internal cross-section.
2. To compute the beam's spanwise structural properties.
3. To determine the first 10 natural frequencies and modes.
4. To evaluate different wing configurations and select a final design based on a performance criteria.

2 Methodology and Code Architecture

2.1 `main` script

The main script of the project is `main.m`, which is the file that must be executed to run the analysis. In it, first, the material properties of the aluminium structure are defined, and then, the design parameters are specified. In particular:

- A vector of candidate spans, `b_vec`.
- A vector of candidate taper ratios, `lambda_vec`.

Additional fixed parameters are also imposed, such as the angle of attack α, the free-stream velocity `U_inf`, and the discretization parameters `Nspan`, `Nx` and `Ny`.

The script loops over all combinations of span and taper ratio and, for each pair (b, λ), calls the function `wing_case`. This function performs the full structural, aerodynamic, and aeroelastic analysis corresponding to that particular wing configuration.

Each case quantities of interest are then stored in the `results` structure array, which serves as the main variable for comparing the different wing designs.

2.2 `wing_case` script

The function `wing_case` is structured into steps, each one responsible for a different part of the structural and aerodynamic analysis, explained hereafter:

STEP 1 - Section properties

The first step computes the cross-sectional properties at the root. Following the structure of the `beam_properties.mlx` script provided by the professor, the geometry is defined as a NACA0010 airfoil, with the constrained root chord and a thickness equal to 10% of the chord. The functions `getMeshData` and `getSectionProperties`, also provided by the professor, are used to generate a finite-element mesh of the airfoil cross-section, assign the material properties, and compute the sectional quantities required by the beam model.

STEP 2 - Spanwise distributions

Once the root section is characterised, it is extended along the span to obtain the full spanwise variation. Parameters such as the wing area S, the aspect ratio AR, and the spanwise chord distribution $c(y)$ are defined here.

Moreover, the function `spanwise_distributions` scales the root properties to each airfoil along the span, assuming geometric similarity. Finally, the corresponding bending stiffness $EI(y)$, torsional stiffness $GJ(y)$, and mass per unit length $m(y)$ are computed and stored in the `span` structure.

STEP 3 - Beam element matrices

As previously mentioned, the structural behaviour of the wing is modelled using a 1D beam model along the span, with three degrees of freedom per node: vertical displacement η, bending rotation ζ, and torsional rotation θ.

The function `beamElementSymbolic` is based on the `euler_bernoulli_beam.mlx` script provided by the professor, and computes the element mass and stiffness matrices symbol-

ically using Hermite shape functions for bending and linear shape functions for torsion. This process generates the following MATLAB functions:

- `beamMass.m`: element mass matrix,
- `beamStiffness.m`: element stiffness matrix,
- `beamForce.m`: element load vector associated with distributed aerodynamic loading.

This symbolic step only needs to be executed once and the resulting files are then called directly during the main analysis.

STEP 4 - Modal Analysis

Afterwards, the function `modal_analysis_wing` assembles the global mass and stiffness matrices and imposes a clamped beam condition at the root by fixing the three degrees of freedom of the first node. It then solves the reduced eigenvalue problem

$$\mathbf{K}_{ff}\boldsymbol{\phi} = \omega^2 \mathbf{M}_{ff}\boldsymbol{\phi},$$

Solving this system yields the natural frequencies and corresponding mode shapes of the wing.

STEP 5 - Aerodynamic Model and Doublet Lattice Method

As pointed, the aerodynamic loads are computed using a Doublet Lattice Method (DLM) based on the `doublet_lattice.mlx` script provided by the professor.

The wing planform is discretised into $N_x \times N_y$ aerodynamic panels, and for each panel:

- The coordinates of the vortex segment endpoints and the collocation point (`x_panel`, `y_panel`) are determined.
- The induced normal velocity at each collocation point, due to all doublet segments, is evaluated using the function `w_doublet`, also provided by the professor.
- The aerodynamic influence coefficient matrix `AIC` is assembled.

Since the studied case is static, with a fixed angle of attack α, the reduced frequency is $k = 0$. Therefore, the reference normal velocity vector `Wref` is simply proportional to α. The linear system

$$AIC \times C_p = -Wref$$

is then solved for the complex pressure coefficient amplitudes `C_p`. Because the case is static, the real part of `C_p` is directly taken as the physical pressure coefficient distribution.

STEP 6 - Lift, Mass and Performance Metrics

Lastly, using the pressure coefficients C_p, the code computes the aerodynamic forces. Each panel area S_{panel} is obtained from the local chord and the spanwise step, and the lift per panel is calculated.

The lift is reshaped into a `Ny` $\times$ `Nx` matrix and integrated along the chord to obtain the spanwise lift distribution `L_span` as a function of the x coordinate. In this way, the total lift L and the lift coefficient C_L can be plotted along the span.

Also, the mass ratio μ is evaluated according to the definition in the assignment.

To finish the analysis, the stresses are evaluated using the first bending-torsion mode. With that, the spanwise variations of the bending rotation $\zeta(y)$ and the torsional rotation $\theta(y)$ are extracted at each structural node. The derivatives $\partial\zeta/\partial y$ and $\partial\theta/\partial y$ are then computed, and using the expression provided in the assignment, the stress distribution $\sigma(y)$ is obtained along the span. The maximum value of this stress distribution, $\sigma_{\max}$, is finally used to compute the non-dimensional stress coefficient C_σ and the stress-to-mass ratio C_σ/μ.

All relevant quantities for each wing configuration (geometry, lift, mass, natural frequencies, and non-dimensional performance metrics) are stored in the `metrics` structure and collected in `results`. Consequently, this allows a comparison between spans and taper ratios, for the final selection.

3 Results

In this section, the different wing configurations tested are presented and compared in terms of their main geometric, structural and aerodynamic parameters. A final design is then selected, and its geometrical characterisation and structural properties are shown.

It must be noted that:

1. The free-stream velocity has been set as $U_\infty = 27$ m/s, which corresponds to approximately 100 km/h, being a representative cruise speed for typical gliders.
2. The angle of attack is set to $\alpha = 4°$, so that the wing operates in the linear range of the lift curve.
3. The geometric design space is explored by varying the semispan b and the taper ratio λ, based on typical values found in glider configurations (`b_vec` = 7-11 m, `lambda_vec` = 0.3-0.6).

The main objective of the study is to identify a wing configuration that provides a high aerodynamic efficiency relative to its structural mass. So, the lift-to-mass ratio

$$\frac{C_L}{\mu}$$

is adopted as the main performance indicator. However, other parameters are monitored to ensure that the selected design remains structurally and aeroelastically acceptable.

3.1 Best candidates

From the full analysis performed over span b and taper ratio λ, Tables 1 and 2 summarize the four wing configurations that showed the higher lift-to-mass ratio.

Table 1: Geometric and mass properties of the best wing configurations analysed.

Case	b [m]	λ	S [m^2]	AR	M_{tot} [kg]	μ
1	9.5	0.30	10.498	34.389	1002.1	28.598
2	10	0.30	11.050	36.199	1054.8	28.598
3	10.5	0.30	11.603	38.009	1107.6	28.598
4	11.0	0.30	12.155	39.819	1160.3	28.598

Table 2: Aerodynamic and structural metrics for the best wing configurations analysed.

Case	C_L	L [N]	C_L/μ	$\sigma_{\max}$ [MPa]	C_σ	C_σ/μ
1	0.548	2621	0.0192	27.333	5714.7	199.8304
2	0.557	2803.9	0.0195	24.668	4899.7	171.3296
3	0.566	2990.5	0.0198	22.375	4232.5	148.0009
4	0.574	3180.6	0.0201	20.387	3681.2	128.7225

From Tables 1 and 2 it can be seen that, in particular, Case 4 shows the highest lift-to-mass ratio, and at the same time, it also has the lowest maximum stress. Although the total lift increases with span, the longer wing distributes its deformation more smoothly, resulting in lower bending and twist curvatures and, consequently, a reduced value of $\sigma_{\max}$. So, for these reasons, Case 4 is selected as the reference wing design.

However, it must be noted that the wing mass is considerably high due to the assumption of a fully solid aluminium cross-section. As a future improvement, the cross section could be redesigned as an airfoil with internal voids or spars, which would reduce the mass.

3.2 Final selected Wing

Table 3 details the geometrical parameters of this wing configuration for the aeroelastic and performance analysis.

Table 3: Geometrical parameters of the selected wing design.

Parameter	Value
Semispan, b [m]	11
Root chord, c_0 [m]	0.85
Tip chord, c_{tip} [m]	0.255
Taper ratio, λ	0.30
Wing area, S [m^2]	12.155
Aspect ratio, AR	39.819
Airfoil	NACA 0010

Structural Properties Along the Span

The spanwise variations of the beam properties for the selected design are:

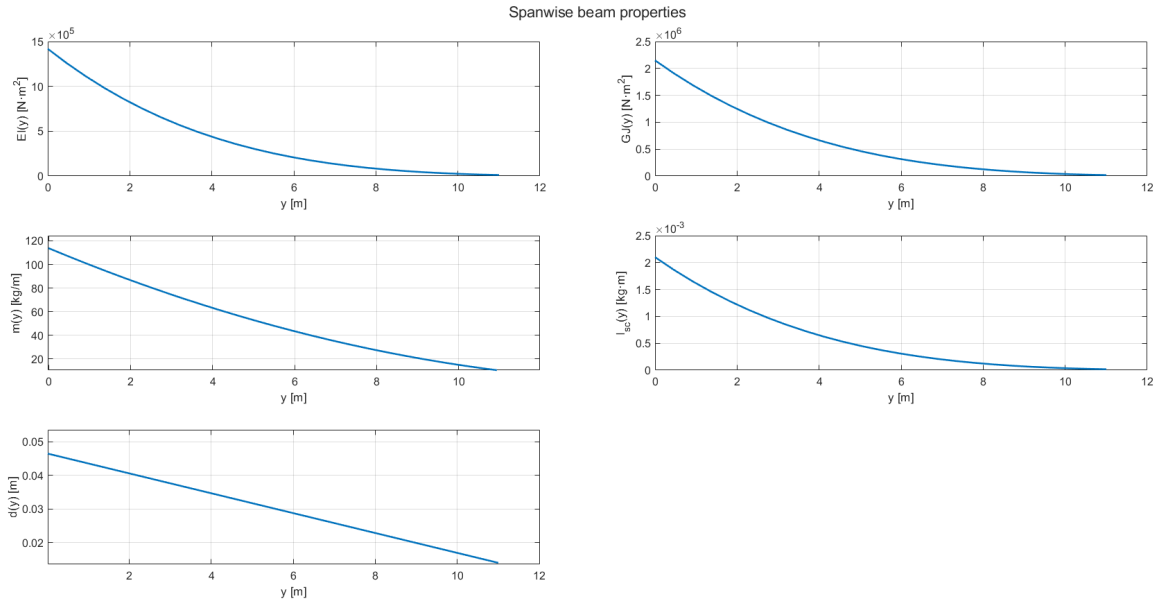

Figure 2: Spanwise variation of the main structural properties for the selected wing.

Which trends are as expected for a tapered wing. Since stiffness and inertia scale strongly with the local chord (c^4), all these quantities decrease rapidly toward the tip. The mass per unit length $m(y)$ also decreases with (c^2), concentrating most of the wing mass near the root. Finally, the offset $d(y)$ between the centre of mass and the shear centre decreases

linearly with the chord.

Natural frequencies and modes

The first ten natural frequencies obtained from the modal analysis of the selected wing design are reported in Table 4, which correspond to the vibration behaviour of the structural model.

Table 4: First ten natural frequencies of the selected wing design.

Mode	**1**	**2**	**3**	**4**	**5**	**6**	**7**	**8**	**9**	**10**
f_i [Hz]	0.808	2.733	6.275	11.510	18.464	27.147	37.567	49.728	63.642	79.321

The corresponding mode shapes are shown in Figure 3. For each mode, the normalised shape of the η, ζ and θ components is displayed along the span.

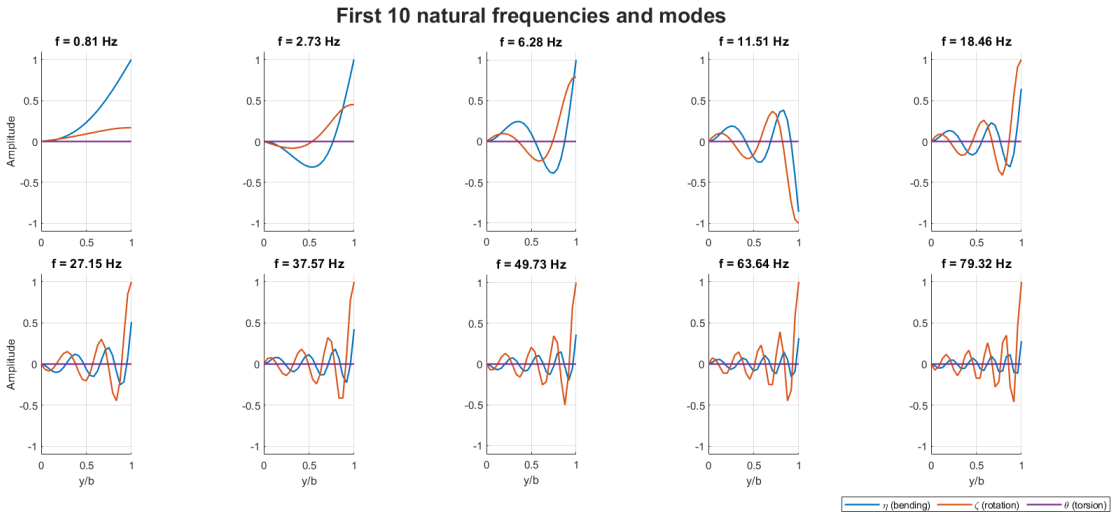

Figure 3: First ten mode shapes of the selected wing design.

As shown, the first modes are dominated by bending. Then, as the mode increases, bending rotation ζ becomes more relevant, while torsion remains almost zero across all the first ten modes, which could be explained by the high torsional stiffness GJ of the solid aluminium cross-section.

Moreover, the first natural frequency is relatively low, which is consistent with the use of a fully solid cross-section. As mentioned earlier, a possible improvement would be to

replace the filled aluminium section with an airfoil containing spars or internal voids, which would reduce the mass while increasing both bending and torsional stiffness.

4 Conclusions

Overall, it can be affirmed that a complete structural and aerodynamic analysis of a tapered glider wing has been performed, exploring a range of spans and taper ratios. Among all the configurations evaluated, the case ($b = 11$ m, $\lambda = 0.30$) has shown the highest lift-to-mass ratio while maintaining the lowest maximum stress, making it the chosen design.

The sectional and spanwise properties have confirmed the expected behaviour of a tapered solid wing, and the natural frequencies have indicated that the first modes are bending-dominated.

However, since a fully solid aluminium cross-section has been assumed, the wing mass is comparatively high. A more realistic wing section incorporating spars or internal voids would significantly reduce the total mass and enhance both bending and torsional stiffness,which could be an improvement for future work.